Available online at www.sciencedirect.com

ScienceDirect

Polymer 49 (2008) 1249–1256

polymer

www.elsevier.com/locate/polymer

Rheological properties of ABA telechelic polyelectrolyte and ABA polyampholyte reversible hydrogels: A comparative study

Nikoletta Stavrouli [a,b], Thierry Aubry [c], Constantinos Tsitsilianis [a,b,*]

[a] Department of Chemical Engineering, University of Patras, 26504 Patras, Greece
[b] Institute of Chemical Engineering and High Temperature Chemical Processes, ICE/HT-FORTH, P.O. Box 1414, 26504 Patras, Greece
[c] Laboratoire de Rhéologie, Université de Bretagne Occidentale, 6 avenue Victor Le Gorgeu, CS 93837 29238 Brest Cedex 3, France

Received 26 October 2007; received in revised form 23 December 2007; accepted 7 January 2008
Available online 15 January 2008

Abstract

Two types of reversible hydrogels formed by poly(*t*-butyl acrylate)–poly(2-vinyl pyridine)–poly(*t*-butyl acrylate) (P*t*BA–P2VP–P*t*BA) and poly(acrylic acid)–poly(2-vinyl pyridine)–poly(acrylic acid) (PAA–P2VP–PAA), named telechelic polyelectrolyte and block polyampholyte, respectively, of the same degree of polymerization were studied in aqueous solutions at pH 3.7 in terms of their rheological properties. The different structural characteristics of the formed 3D networks that arise from hydrophobic interactions of the telechelic polyelectrolyte and electrostatic interactions of the polyampholyte, lead to significant different rheological properties. The results tend to show that a thermo-sensitive weak hydrogel is formed by the polyampholyte while a stiff, but fragile, hydrogel is formed by the telechelic polyelectrolyte.

Keywords: Reversible hydrogel; Telechelic polyelectrolyte; Triblock polyampholyte

1. Introduction

Water-soluble associative polymers forming reversible hydrogels have attracted considerable interest due to their unique rheological properties that make them useful materials as flow modifiers in cosmetics and coatings, injectable hydrogels and drug carriers in pharmaceutical formulations and other waterborn applications [1–4].

Charged associative polymers are either long polyelectrolytes end-capped by hydrophobic blocks, named telechelic polyelectrolytes [5–10], or hydrophilic polyelectrolytes of opposite charges, named block polyampholytes [11,12]. Both types form reversible networks in aqueous systems, named hydrogels, the properties of which are sensitive to pH and ionic strength. Indeed the rheological properties of such hydrogels have been shown to depend much on pH and ionic strength, which influence significantly the conformation of the chains and the topology of the network they form [4,10,11].

The aim of the present work is to compare the rheological properties of the physical hydrogels formed by telechelic polyelectrolytes and triblock polyampholytes with comparable molecular characteristics. The PAA–P2VP–PAA triblock polyampholyte is prepared by acidic hydrolysis of P*t*BA–P2VP–P*t*BA, which is a telechelic polyelectrolyte at low pH since P2VP is a cationic polyelectrolyte at $\mathrm{pH} < 5$, end-capped by hydrophobic P*t*BA blocks. Therefore the two triblock associative polymers under investigation, that is PAA–P2VP–PAA and P*t*BA–P2VP–P*t*BA, exhibit the same degree of polymerization for all the blocks, which allows a relevant comparative investigation.

The P*t*BA–P2VP–P*t*BA telechelic polyelectrolytes associate through hydrophobic interactions of the P*t*BA end-blocks while the PAA–P2VP–PAA polyampholytes associate through electrostatic interactions between the positively charged protonated vinyl pyridine moieties and the negatively charged acrylic acid units. Such differences are expected to

---

* Corresponding author. Department of Chemical Engineering, University of Patras, 26504 Patras, Greece. Tel.: +30 2610 997500; fax: +30 2610 997266.
E-mail address: ct@chemeng.upatras.gr (C. Tsitsilianis).

0032-3861/$ - see front matter © 2008 Elsevier Ltd. All rights reserved.
doi:10.1016/j.polymer.2008.01.015

lead to different network structures, and therefore to different rheological properties of the resulting hydrogels.

2. Experimental part

2.1. Synthesis

P*t*BA–P2VP–P*t*BA triblock copolymer was synthesized by "living" anionic polymerization, using sodium tetraphenyl diisobutane as a bifunctional organometallic initiator, so as to achieve symmetrical chain growth at both active ends. The reaction was carried out in THF solution, under Argon atmosphere at −78 °C and −65 °C, during the addition/reaction of 2-vinyl pyridine and *tert*-butyl acrylate, respectively. The two monomers were distilled twice under vacuum prior to use in order to remove protonic impurities. The 2VP monomer was first distilled over sodium wire and then over calcium hydride after being dried overnight, while the *t*BA monomer was first distilled over calcium hydride, and then treated with triethylaluminium. Each monomer was added to the reactor drop wise. During the addition/reaction of 2VP, the color of the solution changed into dark red and it was followed by the discoloration to pale yellow when a few drops of *t*BA were added. Finally, the reaction was ended by the addition of methanol. The polymer was precipitated in cold hexane, re-dissolved in benzene, filtered and freeze-dried.

The postpolymerization reaction of acid catalyzed hydrolysis of the P*t*BA to PAA blocks was carried out in 1,4-dioxane with 10-fold excess of fuming hydrochloric acid 37% (wt/wt), at 80 °C for 24 h. The degree of hydrolysis was more than 97%. The molecular characteristics of the copolymers under investigation are summarized in Table 1.

2.2. Size exclusion chromatography (SEC)

Size exclusion chromatography was performed, using PL gel columns of different pore sizes and RI-detector, in order to determine the molecular weight distribution of the precursor P2VP and the P*t*BA–P2VP–P*t*BA triblock copolymer. The mobile phase was 1% triethylamine solution in tetrahydrofuran and the flow rate 0.5 ml/min.

2.3. Nuclear magnetic resonance (NMR)

^{1}H NMR spectra were measured on a Bruker AC-400 spectrometer using $CDCl_3$ and d_6-methanol/$CDCl_3$ mixture, as deuterized solvents for precursors (P*t*BA–P2VP–P*t*BA) and hydrolyzed copolymer (PAA–P2VP–PAA), respectively. ^{1}H NMR measurements were used in order to determine the percentage of the different species that constitute the copolymer, as well as the degree of hydrolysis of the final product and the exact molecular weight of both samples. The M_w of the P2VP central block (precursor) was determined by static light scattering.

Table 1
Molecular characteristics of the ABA copolymers

Polymer	M_w/M_n[a]	M_w	P2VP[d] [wt%]	P*t*BA/PAA[d] [wt%]
P2VP	1.14	73 000[b]		
$\text{P}t\text{BA}_{109}$–P2VP_{695}–$\text{P}t\text{BA}_{109}$	1.21	101 000[c]	72.2	27.8
PAA_{109}–P2VP_{695}–PAA_{109}		89 000[c]	82.0	18.0

[a] Measured by SEC.
[b] Measured by SLS in THF.
[c] Calculated from the M_w of P2VP precursor via ^{1}H NMR percentage.
[d] Calculated by ^{1}H NMR.

2.4. Rheometry

The linear and non-linear rheological experiments were performed using two rotational rheometers:

- a stress controlled Rheometrics Scientific SR200 rheometer, equipped with either a cone-and-plate geometry (diameter 25 mm, cone angle 5.7°, truncation 56 μm) or a Couette geometry (gap 1.1 mm) for the less viscous solutions;
- a strain controlled Rheometrics Scientific ARES rheometer, equipped with a parallel-plate geometry (diameter 20 mm, gap 2 mm), for the stress relaxation measurements.

All steady state viscosities were determined as limits of the transient viscosities following the criterion: time evolution of the transient viscosity lower than 1% during 1 min.

A thin layer of low viscosity silicone oil was put on the air-sample interface in order to minimize water evaporation. After each sample loading, normal force was monitored, and no measurement was carried out before complete relaxation of the sample. Most rheological tests presented in the paper were performed at 25 °C, but temperature effects were specifically studied over a temperature range from 25 °C to 55 °C.

2.5. Sample preparation

Dissolution was performed at room temperature (20–25 °C) in order to avoid any hydrolysis reaction of P*t*BA blocks that could occur at high temperature under acidic environment. Although the T_g of P*t*BA blocks (52 °C as determined by DSC) is higher than room temperature, we did not face solubility problems as reported for PS–PAA–PS telechelic polyelectrolytes, where prolonged heating was needed to prepare homogeneous gels. Gel homogenization was achieved mechanically by rigorous stirring. As shown below (see Fig. 4a), the gel is quite fragile, which permits rearrangements of the involving macromolecules needed for the network formation.

For all samples tested, pH was fixed at 3.7 in order to ensure the existence of both polyampholyte character for PAA–P2VP–PAA copolymer (co-existence of both positive and negative charges along the polymer chain with isoelectric point at pH 5.6) and polyelectrolyte character for P*t*BA–P2VP–P*t*BA. From zeta potential and optical density versus pH curves it was shown that pH 3.7 lies below the isoelectric point region ($4.8 < \text{pH} < 6.8$) in which the polyampholyte precipitates due to electrostatic neutralization of the oppositely charged moieties and P2VP deprotonation [11].

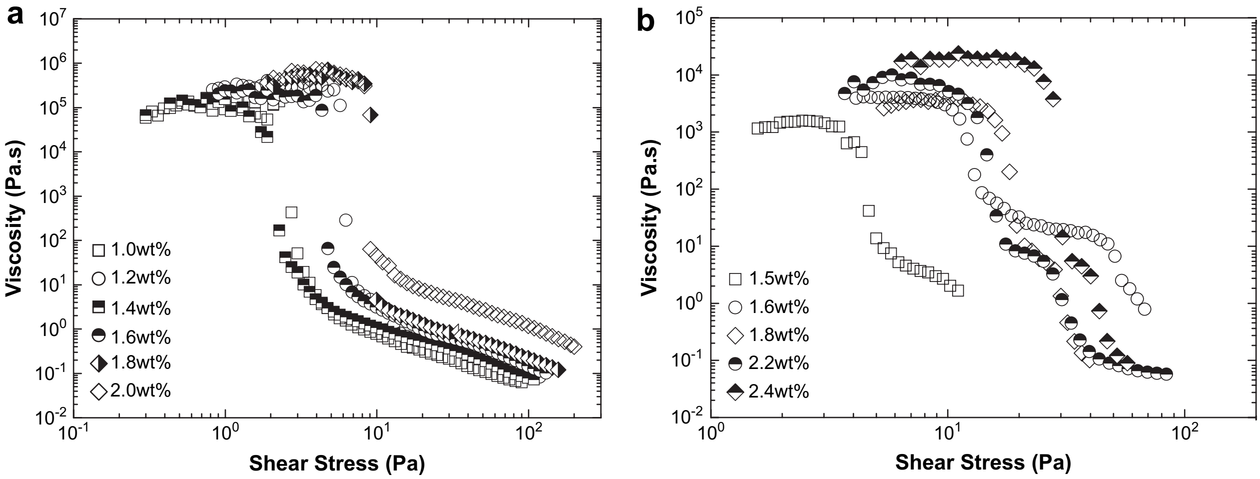

Fig. 1. Apparent viscosity as a function of shear stress for: (a) the polyelectrolyte P*t*BA–P2VP–P*t*BA, over a concentration range from 1.0 to 2.0 wt% and (b) the polyampholyte PAA–P2VP–PAA, over a concentration range from 1.5 to 2.4 wt%.

3. Results

At pH 3.7, the dissolved P2VP block is expected to be protonated, thus exhibiting a stretched conformation [13]. In the case of telechelic polyelectrolyte it is obvious that P*t*BA–P2VP–P*t*BA is aggregated through the P*t*BA hydrophobic stickers, forming macroscopically an infinite network through hydrophobic interactions [9]. On the contrary, in the case of the PAA–P2VP–PAA polyampholyte the network formation is due to the electrostatic (Coulombic) interactions between the oppositely charged repeating units [12].

3.1. Steady shear

Fig. 1a and b, shows the flow curves of the telechelic polyelectrolyte (P*t*BA–P2VP–P*t*BA) and of the polyampholyte (PAA–P2VP–PAA), respectively. Firstly, both polymeric systems exhibit a classical flow curve at low concentrations that is a low-shear Newtonian plateau followed by a smooth shear-thinning behaviour at higher shear rates. Above a polymer concentration, whose value depends on the system, the flow curve of both systems exhibits either one (for polyelectrolyte) or two (for polyampholyte) drastic shear-thinning regions. This kind of strong non-linear behaviour, corresponding to discontinuities in the viscosity versus shear stress curve, has been observed with other network forming associative polymeric systems [14,15]. It is worth noticing that the second drastic shear-thinning region, and the intermediate "plateau" (i.e. the region between the two abrupt shear-thinning regimes) are more or less marked, according to the polymeric system and concentration.

The zero-shear Newtonian viscosity as a function of polymer concentration is shown in Fig. 2, for both systems. First, the viscosity level of the polyelectrolyte (P*t*BA–P2VP–P*t*BA) far exceeds that of the polyampholyte (PAA–P2VP–PAA) at any concentration. Moreover, the viscosity versus concentration curve exhibits three distinct regions for both systems, as observed in many associative polymeric systems [5,7,9,12]:

- a "semi-dilute" regime, where viscosity increases weakly with polymer concentration, following a power law $\eta \sim C^a$, where $a \sim 0.6$ for the telechelic polyelectrolyte, and $a \sim 0.4$ for the polyampholyte. These exponents are in relatively good agreement with the theoretical scaling exponent for semi-dilute polyelectrolyte solutions [20];
- above a concentration threshold, denoted as C_{gel}, a region where the viscosity exhibits a very sharp increase over a very limited concentration range, which may even look like a discontinuity in the case of the polyampholyte system;
- at higher concentrations, a regime where the viscosity smoothly increases with concentration.

The concentration threshold, C_{gel}, characteristic of a gelation process, is about 6×10^{-3} g/ml for the polyelectrolyte and 11×10^{-3} g/ml for the polyampholyte. If the critical concentration of gelation is expressed in mol/ml, which is a more

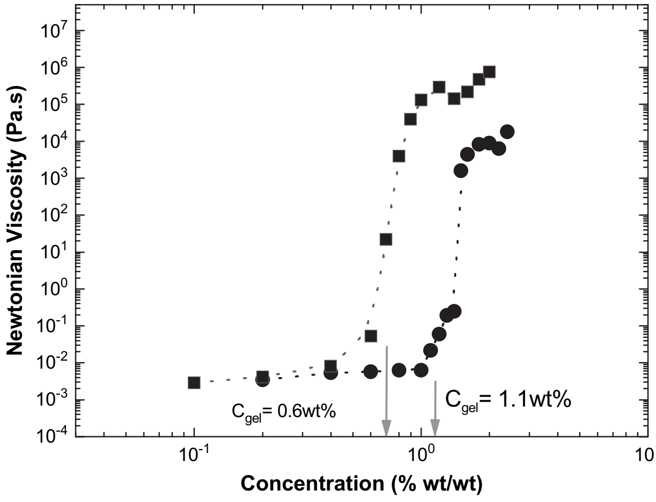

Fig. 2. Double logarithmic plot of the zero-shear viscosity, η_0, as a function of concentration for P*t*BA–P2VP–P*t*BA (■) and PAA–P2VP–PAA (●), in acidic aqueous solution (pH = 3.7) at 25 °C. Determination of critical concentration of gelation, C_{gel}.

relevant concentration unit, then the critical concentration of gelation turns out to be 5.95×10^{-5} mol/ml for the polyelectrolyte and 1.23×10^{-4} mol/ml for the polyampholyte. So the polyampholyte chains are twice as numerous as the polyelectrolyte chains at the gelation concentration threshold.

The apparent yield stress, σ_y, which is defined as the stress marking the transition from a low-shear Newtonian behaviour to a drastic shear-thinning behaviour (cf. Fig. 1a and b), is plotted as a function of concentration in Fig. 3, for both systems. Fig. 3 shows that the apparent yield stress of the polyampholyte system is higher than that of the polyelectrolyte, except at the lowest concentrations, where marked deviations from the general trend are observed. Moreover, the yield stress of the polyampholyte system increases more strongly with concentration than that of the polyelectrolyte system. Indeed, for both systems, leaving out the data at the lowest concentrations, which would need additional investigation in order to be discussed, a power law function, $\sigma_y \sim c^a$, can be used, with $a \sim 1.2$ for the polyelectrolyte system and $a \sim 2$ for the polyampholyte system.

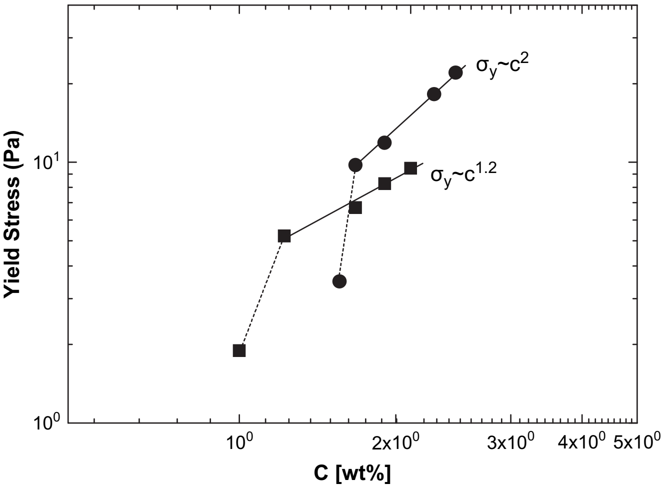

Fig. 3. Apparent yield stress as a function of concentration of both polyelectrolyte (■) and polyampholyte (●). Solid lines represent linear fits.

3.2. Oscillatory shear

The storage and loss moduli as a function of strain are plotted in Fig. 4a for the polyelectrolyte system and Fig. 4b for the polyampholyte system, at different concentrations. All measurements were performed at 0.5 Hz. There are two major differences in the viscoelastic properties of the two systems, regarding their strain dependency:

- the extent of the linear viscoelastic regime is small, limited to strains inferior to 0.5% in the case of the polyelectrolyte system, whereas it is rather large, up to strains ~50%, for the polyampholyte system;
- the non-linear viscoelastic behaviour of the polyelectrolyte system is characterized by a continuous decrease of both viscoelastic moduli, whereas both G' and G'' exhibit a strain hardening followed by a strain thinning behaviour in the case of the polyampholyte system. The existence of such a non-linear viscoelastic profile, characterized by peak in G' and G'' as a function of strain, has been observed with other associative polymeric systems [16].

The linear viscoelastic moduli of a 2 wt% polymer solution as a function of frequency are plotted in Fig. 5 for the two polymeric systems of interest in this work. It is worth reminding that a 2 wt% concentration lies in the upper concentrated regime for both systems. At such a polymer concentration, where the network is fully developed, the two types of polymeric systems exhibit a significant difference in frequency dependency of G' and G'':

- the polyelectrolyte system exhibits nearly frequency independent viscoelastic moduli, with $G' > G''$, corresponding to solid-like behaviour;
- the polyampholyte system exhibits a tendency to relax on long time scales (cf. behaviour at low frequencies), even though $G' > G''$ over a large frequency range.

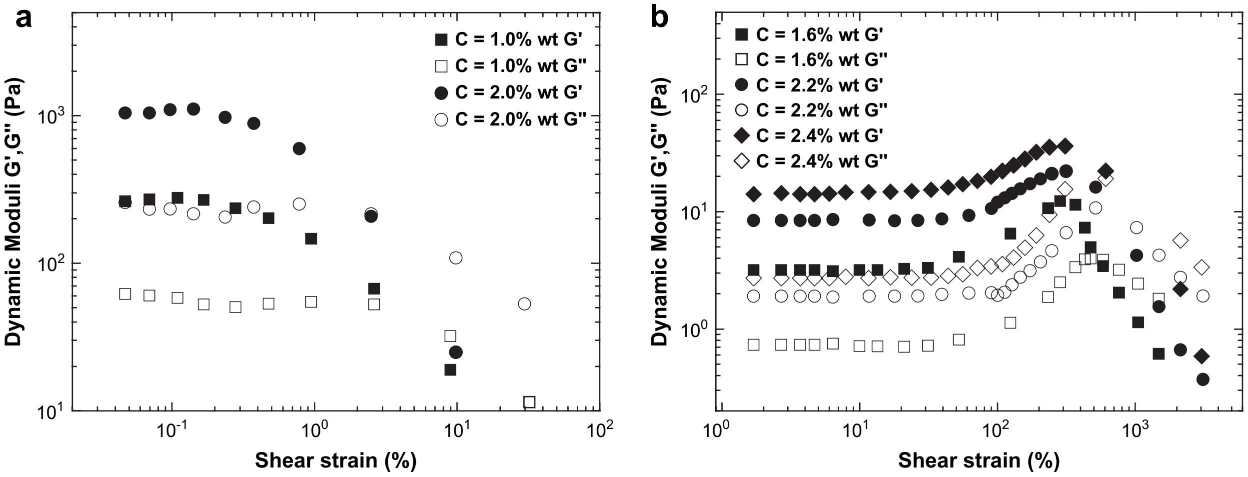

Fig. 4. Storage modulus G' (■, ●, ◆) and loss modulus G'' (□, ○, ◇) for several concentrations, as a function of % shear strain, at 25 °C, for both polyelectrolyte (a) and polyampholyte (b).

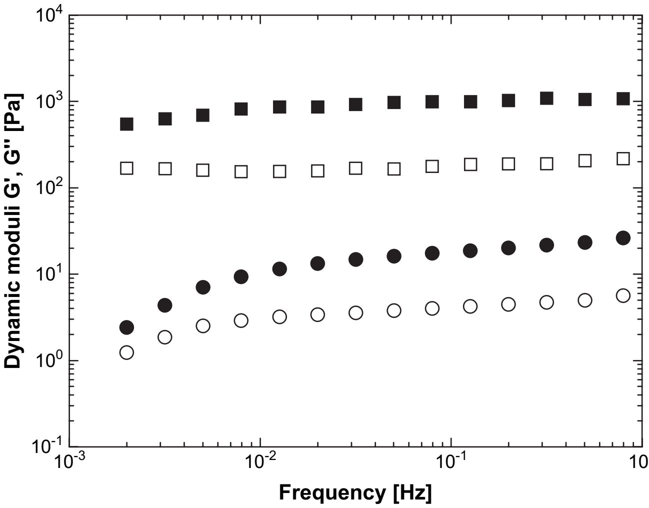

Fig. 5. Storage modulus G' (■, ●) and loss modulus G'' (□, ○) for the same concentration (2.0 wt%) for the polyelectrolyte (■, □ P*t*BA–P2VP–P*t*BA) and the polyampholyte (●, ○ PAA–P2VP–PAA), as a function of frequency at 25 °C.

In order to make a more quantitative comparison of the elastic energy stored in the network of the two systems, the plateau value of G', denoted as G'_0, that is the value determined in the region where the storage modulus is nearly independent of frequency, has been plotted as a function of concentration, in Fig. 6. First of all, at any given polymer concentration, the elasticity of the polyampholyte system is much weaker than that of the polyelectrolyte system. Besides, for both systems, G'_0 is a power law function of concentration: $G'_0 \sim C^a$, where $a = 1.7$ for the polyelectrolyte system and $a = 3.8$ for the polyampholyte system.

The difference in the dependence of the plateau elastic modulus with polymer concentration between polyelectrolyte system and polyampholyte one, is the signature of a difference in network topology. Indeed, the transient network theory predicts that the plateau modulus is given by: $G'_0 = \nu k_B T$, where ν is the number density of elastically effective chains [21], and thus predicts that G'_0 will increase linearly with concentration, if all polymer chains do act as bridging chains. Therefore the fact that the power law exponent is much closer to unity for the polyelectrolyte than for the polyampholyte means that the probability of forming bridges is much higher in the polyelectrolyte system, even though loops, dangling ends, so-called ‘‘superbridges’’ and ‘‘superloops’’, in the language of Annable et al. [22], may be present. For a more quantitative insight into the topology of both gels, let us evaluate the fraction of elastically active chain, $G'_0/Nk_B T$, where N is the number density of polymer chains, for both systems at 2 wt%. Using the data presented in Fig. 5, the fraction of elastically active polyelectrolyte chains is found to be slightly higher than 1, whereas that of elastically active polyampholyte chains is found to be ∼10%.

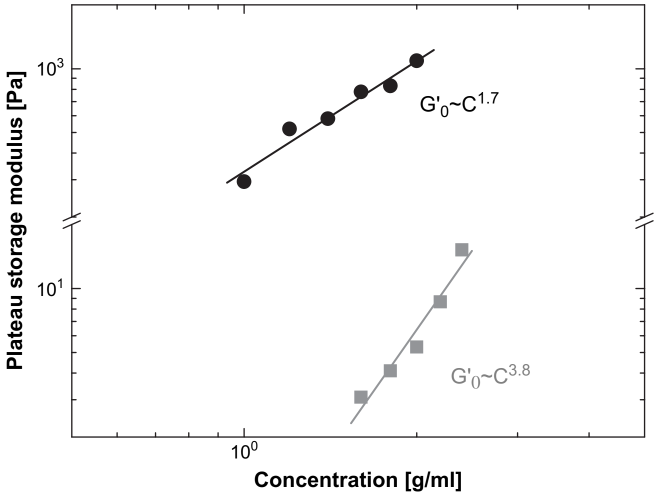

Fig. 6. Plateau storage modulus as a function of concentration of both polyelectrolyte (●) and polyampholyte (■). Lines represent linear fits.

3.3. Stress relaxation

The stress relaxation modulus as a function of time is plotted in Fig. 7, for both polymeric systems, at a 2 wt% concentration. There is a clear qualitative difference in relaxation behavior between the two systems:

- the stress relaxation modulus of the polyelectrolyte exhibits a power law decay with time, $G(t) = G_0 t^{-\Delta}$, where the instantaneous elastic modulus $G_0 \sim 1000$ Pa, and the exponent $\Delta \sim 0.2$;
- for the polyampholyte system, the best fit of the stress relaxation response is obtained with a stretched exponential function, $G(t) = G_0 \exp(-t/\tau)^{\alpha}$, where the instantaneous elastic modulus $G_0 \sim 30$ Pa, the exponent $\alpha \sim 0.2$, and the characteristic time $\tau \sim 120$ s.

3.4. Temperature effect

Finally the influence of temperature on the steady state shear viscosity was explored for both systems. In Fig. 8 the

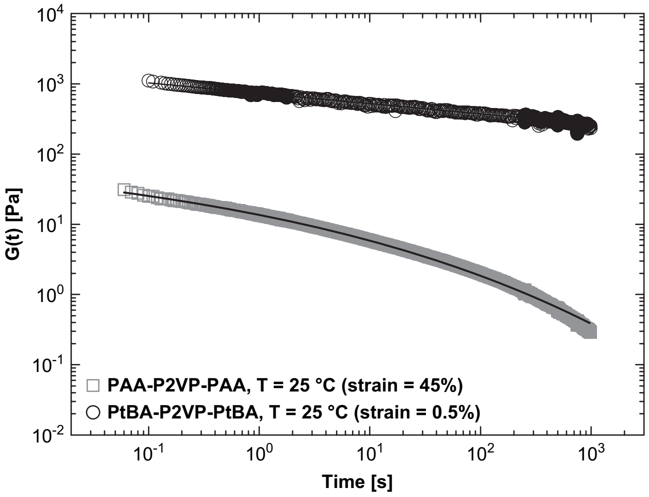

Fig. 7. Stress relaxation modulus of a 2 wt% polymer solution at 25 °C for strain amplitudes γ of 0.5% for P*t*BA–P2VP–P*t*BA and 45% for PAA–P2VP–PAA. The continuous lines through data represent the best-fitting calculation curves.

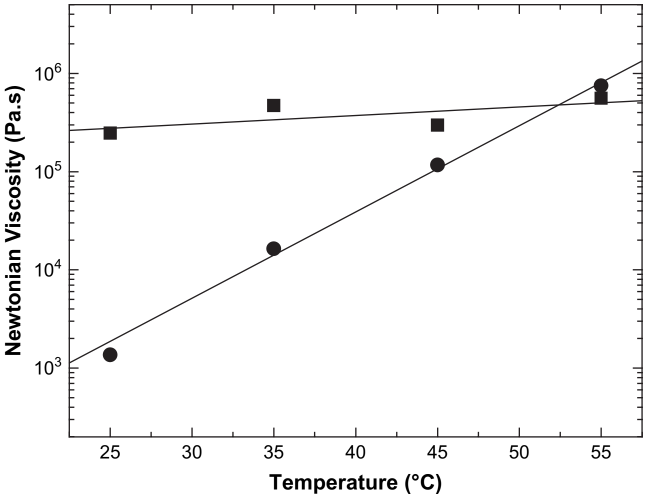

Fig. 8. Newtonian viscosity as a function of temperature for 2 wt% solutions of polyelectrolyte (■) and polyampholyte (●). Lines are provided to guide the reader.

Newtonian viscosity of the two samples is plotted as a function of temperature. It shows significantly different behavior for the two systems. For the polyampholyte, the temperature increase from 25 °C to 55 °C results in a three-decade increase of the Newtonian viscosity. On the contrary, the viscosity in the telechelic polyelectrolyte remains independent of temperature. The smooth viscosity increase must be considered negligible.

4. Discussion

The rheological results indicate significant quantitative and qualitative differences in the behavior of the reversible hydrogels formed from the two different associative polymers studied in this work. In order to better understand and compare these results, the expected differences between the two systems, regarding intramolecular and intermolecular interactions, chain conformations and 3D network structure should be pointed out first.

The association process for the telechelic polyelectrolyte is governed by the competition between the attractive hydrophobic interactions of the sticky outer blocks and the repulsive electrostatic interactions along the hydrophilic polyelectrolyte middle block. At low concentrations, the hydrophobic interactions between the outer blocks seem to overcome the repulsive interactions along the middle chain, leading to the formation of flower like micelles [7,9]. Above a certain concentration, the electrostatic interactions favor loop to bridge transitions leading to the formation of a 3D physical network with significant higher fraction of bridging chains with respect to the non-ionic associative telechelic polymers [6] (see Fig. 9a and b). Moreover, the elastic chains adopt an extending conformation which is expected to have major consequences on the rheological properties.

On the other hand the polyampholyte system exhibits a different association mechanism. The character of the polymer under investigation is double hydrophilic (lack of hydrophobic stickers). The transient network is mainly composed of

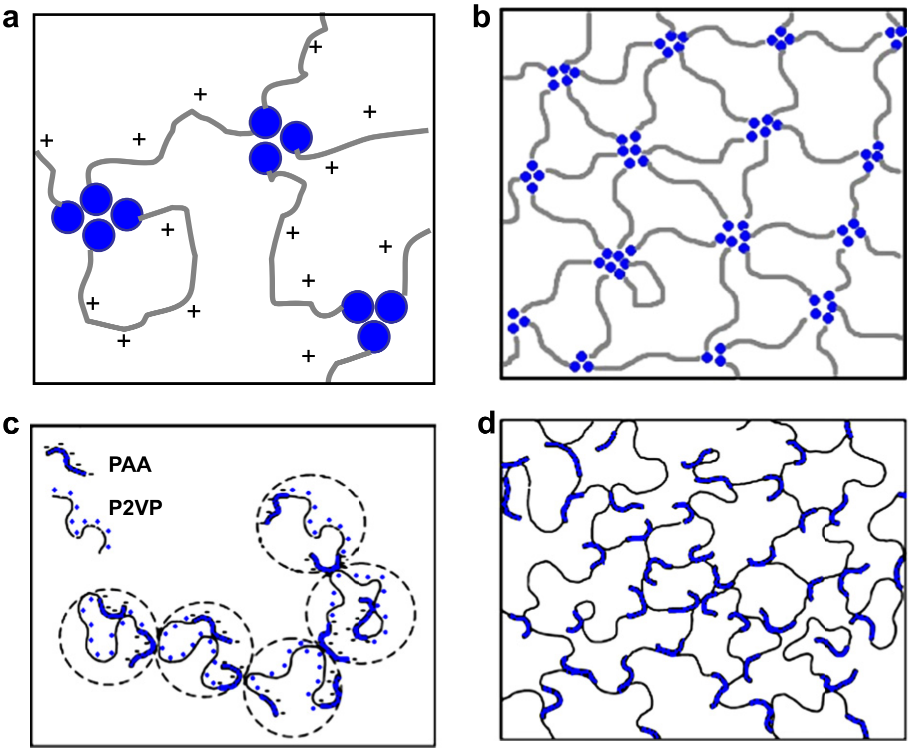

Fig. 9. Schematic representation of the formation of 3D transient network from P*t*BA–P2VP–P*t*BA through hydrophobic interactions (a,b) and PAA–P2VP–PAA through electrostatic interactions (c,d).

elastically active chains that arise from intermolecular electrostatic interactions between the negatively charged groups located in the outer PAA blocks and the positively charged located in the middle long P2VP block (Fig. 9c and d). Intramolecular associations are likely to occur since, at pH 3.7, the long P2VP chains do not adopt exclusively a stretched conformation, as reported recently [12], and also a number of PAA block ends may stay unassociated forming dangling ends, as they are water soluble, contrary to what occurs in hydrophobically associative polymers. Therefore, there are a number of elastically inactive chains (dead branches for the network) that nevertheless can be considered as potentially active, becoming effective under shear. The electrostatic associations should also decrease the extension of the P2VP chains (less stretched conformations with respect to those of telechelic polyelectrolytes) due to the neutralization of the charges along the chain.

Taking into consideration the above-discussed expected differences between the two systems, regarding intramolecular and intermolecular interactions, chain conformations and 3D network structures, we would now like to discuss the rheological results.

First of all, it is quite clear that, above a critical concentration denoted as C_{gel}, both systems have a gel-like behaviour, due to the formation of a three-dimensional physical network. Indeed the gel-like behaviour is exhibited in many features of the linear and non-linear rheological response to shear of the two systems, above C_{gel}:

- the drastic increase of the zero-shear Newtonian viscosity at $C_{\text{gel;}}$
- the existence of an apparent yield stress;
- the existence of near discontinuities in the flow curves;
- the predominant elastic contribution to the linear viscoelastic response;
- the weak dependence of the storage and loss moduli on the frequency.

However, much more interestingly, there are also quite significant differences in linear and non-linear rheological behaviours between the two polymeric networks studied in this work that we would like to discuss in terms of macromolecular properties.

The first qualitative and quantitative differences concern with the strain dependence of viscoelastic moduli: the extent of linear viscoelastic regime and also the qualitative features in G' and G'' vs. strain curves. We think that these differences may be attributed mainly to differences in chain conformation. Indeed we suggest that the polyampholyte system has a larger linear viscoelastic domain than that of the polyelectrolyte because of the larger stretchability of P2VP central blocks in the polyampholyte. The relative "fragility" of the polyelectrolyte network is also exhibited in the lower value of the yield stress of the polyelectrolyte compared to that of the polyampholyte system, at the same concentration.

Besides, the existence of a peak in G' vs. strain curves for the polyampholyte could be attributed not only to stretchability of the P2VP chains (non-linear effects at large extensions), but also to the strain-induced formation of many new connections, involving both dangling chains and chains involved in intramolecular interactions, leading to an increase of number density of elastically active chains within the network.

The existence of many dangling chains in the polyampholyte system, which are expected to be inexistent in the polyelectrolyte, also results to major differences in both the ability of forming a 3D network and the topology of the network, once formed. Indeed, as shown previously in the paper, if twice more macromolecules are needed to form a network at the percolation threshold for the polyampholyte compared to the polyelectrolyte of the same macromolecular characteristics, it means that the elastic strands they can form are different, and that their number density in the network will be different too. In the case of polyampholyte, some elastic strands may be composed of one, two, or even more, macromolecules (Fig. 9c), depending on the polymer concentration. This could explain the significant differences in the dependence of the linear elastic modulus and the yield stress with polymer concentration of both polymeric systems, but it could also contribute to explain why, at the same concentration, the polyampholyte network stores less elastic energy and is less resistant to flow than the polyelectrolyte network. More precisely, the more abrupt increase of G'_0 with concentration on the polyampholyte, implies rearrangements of elastic strands to elastically active chains as well as further association of dangling PAA ends which both increases the overall number density of the elastic chains.

Finally, the difference in stress relaxation behavior, at a given concentration, has its origin, most likely, in differences in network topology, giving the polyelectrolyte the characteristics of a strong stiff critical gel, and the polyampholyte the characteristics of a soft weak gel.

At last the temperature sensitivity of the polyampholyte system may be attributed to temperature induced changes of conformation of PAA blocks. More precisely PAA exhibits Θ point (UCST) at 14 °C in 0.2 M HCl aqueous solutions [17]. Provided that the ionic strength is low but not zero, the Θ point could be slightly higher. At low temperatures the PAA end-blocks shrink and do not play any significant role in the network connectivity (dangling ends). As temperature increases, PAA swelling gives rise to the development of intermolecular electrostatic interactions among oppositely charged repeating units which leads to an increase in the elastic chains of the network (dangling end to crosslink transitions) and therefore to a significant viscosity augmentation [18]. H-bonding between uncharged 2VP and AA units may also exist, but does not seem to play important role in the thermo-thickening behavior at pH 3.7. Otherwise this phenomenon should exist also at pH 2, where H-bonding is more favorable (fully protonated AA units) [19]. Moreover, a temperature increase should destroy such H-bonds and should induce an opposite effect. However, intramolecular H-bonding existing between acrylic units (the degree of ionization is very low at pH 3.7) should break upon heating, favoring the intermolecular contacts among the P2VP and PAA blocks and therefore the electrostatic interactions responsible for the thermo-thickening effect.

On the other hand, the polyelectrolyte system remains stable against temperature, which has also been observed in PS–PAA–PnBMA water system at pH 7, where the polymer behaves as telechelic polyelectrolyte [7]. This interesting behavior should be ascribed to the stability of the 3D network and more precisely to the glassy and hydrophobic character of the P*t*BA physical crosslinks. In fact, it is a ''frozen'' system (out of thermodynamic equilibrium) since the mobility of the P*t*BA stickers is close to zero. This is also consistent with the elastic behavior of the gel (relaxation time higher than 1000 s) as depicted in Fig. 5.

5. Conclusions

We have presented a comparative rheological study of two different types of hydrogels, based on telechelic polyelectrolyte (P*t*BA–P2VP–P*t*BA) and polyampholytic system (PAA–P2VP–PAA) of similar molecular characteristics. With both systems, a three-dimensional network is formed above a critical gelation concentration, but significant quantitative and qualitative differences in the behavior of the reversible hydrogels formed from the two associative polymers were observed. The differences in linear and non-linear rheological properties of the two systems were attributed to differences in intramolecular and/or intermolecular interactions, resulting, in differences in chain conformation and, finally in 3D network structure. The fact that P2VP central chains do not adopt exclusively a stretched conformation and that a number of PAA block ends may form dangling ends in the polyampholyte, and not in polyelectrolyte, could play a key role by inducing differences in the topology and mechanical properties of the network of these two systems. All the results tend to show that, at a given polymer concentration, the structure of the polyampholyte, governed by electrostatic interactions, is that of a weak physical gel, whereas the structure of the polyelectrolyte, mainly governed by hydrophobic interactions, is rather that of a stiff, but fragile, physical gel.

As a conclusion, we think that the rheological properties of the polyampholyte system, in combination with its convenient dilution in aqueous media, its sensitivity to external stimuli, like temperature, and other properties that have not been discussed in the paper, make the double hydrophilic polyampholyte copolymer a very interesting system as far as applications are concerned.

Acknowledgement

The present work was performed within the framework of the 2006/2007 French–Greek ''Platon'' PHC Project no.11299 RH. T. Aubry acknowledges financial support of the French Ministry of Foreign Affairs. N. Stavrouli would like to thank the Greek Ministry of Development for the financial support of her stay in the University of Brest.

References

[1] Winnik MA, Yekta A. Curr Opin Colloid Interface Sci 1997;2:424.
[2] Rubinstein M, Dobrynin AV. Curr Opin Colloid Interface Sci 1999;4:83.
[3] Berret J-F, Calvet D, Collet A, Viguier M. Curr Opin Colloid Interface Sci 2003;8:296.
[4] Kimerling AS, Rochefort WE, Bhatia SR. Ind Eng Chem Res 2006;45:6885.
[5] Tsitsilianis C, Iliopoulos I, Ducouret G. Macromolecules 2000;33:2936.
[6] Tsitsilianis C, Iliopoulos I. Macromolecules 2002;35:3662.
[7] Katsampas I, Tsitsilianis C. Macromolecules 2005;38:1307.
[8] Katsampas I, Roiter Y, Minko S, Tsitsilianis C. Macromol Rapid Commun 2005;26:1371.
[9] Stavrouli ND, Tsitsilianis C, Kiriy A, Gorodyska G, Stamm M. J Nanostruct Polym Nanocomp 2005;1:15.
[10] Bossard F, Aubry T, Gotzamanis GT, Tsitsilianis C. Soft Matter 2006:510.
[11] Sfika V, Tsitsilianis C. Macromolecules 2003;36:4983.
[12] Bossard F, Sfika V, Tsitsilianis C. Macromolecules 2004;37:3899.
[13] Roiter Y, Minko S. J Am Chem Soc 2005;127:15688.
[14] Berret JF, Séréro Y. Phys Rev Lett 2001;87:483031.
[15] Berret JF, Séréro Y, Winkelman B, Calvet D, Collet A, Viguier M. J Rheol 2001;45:477.
[16] Tirtaatmadja V, Tam KC, Jenkins RD. Macromolecules 1997;30:1426.
[17] Silberberg A, Eliassaf J, Katchalsky A. J Polym Sci 1957;23:259.
[18] Bossard F, Tsitsilianis C, Yannopoulos S, Petekidis G, Sfika V. Macromolecules 2005;38:2883.
[19] Stavrouli N, Katsampas I, Aggelopoulos S, Tsitsilianis C. Macromol Rapid Commun 2008;29:130.
[20] Dobrynin AV, Colby RC, Rubinstein M. Macromolecules 1995;28:1859.
[21] Green MS, Tobolsky AV. J Chem Phys 1946;14:80.
[22] Annable T, Buscall R, Ettelaie R, Whittlestone D. J Rheol 1993;37:695.